Gas-Phase Structure of the Monomeric Alkylgallium(I) Compound $Ga[C(SiMe_3)_3]$ and the Electrochemical Behavior of $Ga_4[C(SiMe_3)_3]_4$ and $In_4[C(SiMe_3)_3]_4$ with EPR Evidence for a Ga_4R_4 Radical Anion

Arne Haaland, Kjell-Gunnar Martinsen, and Hans Vidar Volden

Department of Chemistry, University of Oslo, Box 1033 Blindern, N-0315 Oslo, Norway

Wolfgang Kaim and Eberhard Waldhör

Institut für Anorganische Chemie der Universität Stuttgart, Pfaffenwaldring 55, D-70550 Stuttgart, Germany

Werner Uhl* and Uwe Schütz

Fachbereich Chemie der Universität, Postfach 25 03, D-26111 Oldenburg, Germany

Received September 25, 1995[⊗]

The gallium(I) compound $Ga_4[C(SiMe_3)_3]_4$ (**1**) with a tetrahedral Ga_4 core in the solid state gives on evaporation the monomeric Ga(I) alkyl $Ga[C(SiMe_3)_3]$ with the unique structural situation of a Ga atom solely coordinated by one singly bonded carbon ligand. Its molecular structure was determined now by gas-phase electron diffraction yielding a Ga−C bond length of 206.4(17) pm, similar to that found in the solid state for the tetramer and much longer than in compounds with gallium in the normal oxidation state of +3. As shown by cyclic voltammetry, **1** and the analogous cluster $In_4[C(SiMe_3)_3]_4$ (**2**) could both be reversibly reduced at about −2 V vs $Fc^{+/0}$. Whereas the reduced organoindium tetramer did not exhibit any detectable EPR signals between 4 and 300 K, the gallium analogue showed an EPR spectrum compatible with the formulation $[(RGa^{0.75})_4]^{\bullet-}$; i.e. the unpaired electron was found to be delocalized over all four metal centers ($a(^{69}Ga) = 1.93$ mT, $a(^{71}Ga) = 2.45$ mT, 4 Ga).

Introduction

Recently we synthesized the first published alkylgallium(I) derivative $Ga_4[C(SiMe_3)_3]_4$ (**1**) via the reaction of $Ga_2Br_4 \cdot 2$dioxane with unsolvated $LiC(SiMe_3)_3$ (eq 1).[1] In the solid state **1** exhibits a nearly undistorted

$$Ga_2Br_4 \cdot 2\ \text{dioxane} + 3\ LiC(SiMe_3)_3 \rightarrow 1/n\ [Ga\text{-}C(SiMe_3)_3]_n + \text{"}BrGa[C(SiMe_3)_3]_2\text{"} + 3\ LiBr + 2\ \text{dioxane} \quad (1)$$

1 (n = 1 or 4)

tetrahedral core of four Ga atoms, but in dilute benzene solution it becomes a monomer, as shown by the cryoscopically determined molar mass. The monomer is further detected by conventional mass spectroscopy as the highest observed mass peak. From eq 1 a monobromo derivative is expected as the second product of the disproportionation reaction; instead, a mixture of several unknown products is formed.

The In_4 analogue (**2**) was synthesized via another route starting with InBr and $LiC(SiMe_3)_3 \cdot 2THF$ (eq 2),[2] similar to a procedure independently given by

$$4\ InBr + 4\ LiC(SiMe_3)_3 \cdot 2\ THF \rightarrow In_4[C(SiMe_3)_3]_4 + 4\ LiBr + 8\ THF \quad (2)$$

2

Cowley and co-workers.[3] Again, a crystal structure determination reveals a nearly undistorted tetrahedral In_4C_4 center,[2] but in contrast to **1,** the tetraindane **2** remains tetrameric in dilute benzene solutions. While the tetrameric formula unit is found in FD mass spectra, only the monomer is detected with conventional techniques. In the course of systematic investigations of the chemical and physical properties of these unique compounds we determined the gas-phase structure of the monomeric alkylgallium(I) derivative and investigated some electrochemical properties of the cluster compounds **1** and **2**.

Experimental Section

Electron Diffraction. Gas-phase electron diffraction data were recorded on a Balzers Eldigraph KDG-2 unit[4] with a conventional metal inlet system. Ga_4R_4 is thermally stable to 255 °C in glass containers,[1] but the thermal stability in the presence of metal surfaces has not been studied. Every effort was therefore made to record the diffraction data at the lowest possible temperature. Small-angle scattering data were collected with a nozzle to plate distance of about 50 cm and nozzle and chamber temperatures of about 150 °C, corresponding to an estimated vapor pressure of about 0.05 Torr.

Wider angle scattering data were recorded with a nozzle to plate distance of about 25 cm. Unfortunately, it proved necessary to increase the chamber and nozzle temperatures to about 200 °C in order to obtain sufficient scattering intensity. After initial structure refinements had indicated significant differences between the 50 and 25 cm data in the range below $s = 100$ nm^{-1}, we made yet another attempt on recording 25 cm data at lower temperature but without success.

[⊗] Abstract published in *Advance ACS Abstracts,* January 15, 1996.

(1) Uhl, W.; Hiller, W.; Layh, M.; Schwarz, W. *Angew. Chem., Int. Ed. Engl.* **1992**, *31*, 1364.

(2) Uhl, W.; Graupner, R.; Layh, M.; Schütz, U. *J. Organomet. Chem.* **1995**, *493*, C1.

(3) Schluter, R. D.; Cowley, A. H.; Atwood, D. A.; Jones, R. A.; Atwood, J. L. *J. Coord. Chem.* **1993**, *30*, 25.

(4) Zeil, W.; Haase, J.; Wegmann, L. *Z. Instrumentk.* **1966**, *74*, 84.

0276-7333/96/2315-1146$12.00/0

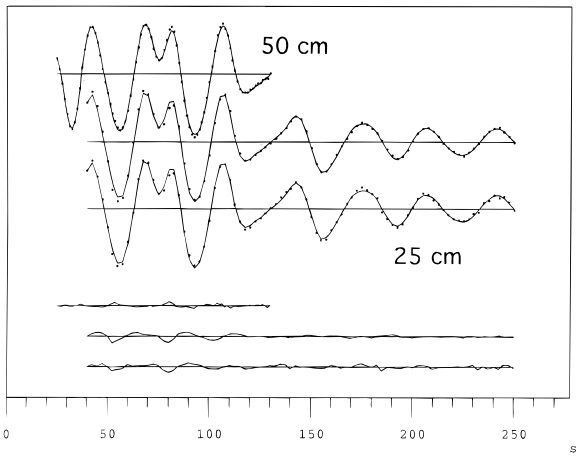

Figure 1. Experimental (dots) and calculated (lines) modified molecular intensity curves for GaC*{Si(CH$_3$)$_3$}$_3$. The vertical scale is arbitrary. Below: Difference curves.

The final structure refinements were based on three plates recorded with a nozzle to plate distance of 50 cm and two and three plates, respectively, from the two sets of plates recorded with a distance of 25 cm. The plates were photometered on a modified Joyce-Loebl microdensitometer and processed with a program written by Strand. Atomic scattering factors were taken from ref 5. Backgrounds were drawn as least-squares adjusted polynomials to the difference between total experimental and calculated molecular intensities. The resulting modified molecular intensity curves are shown in Figure 1.

Cyclic Voltammetry and EPR. EPR spectra were recorded in the X band on a Bruker System ESP 300E equipped with a Bruker ER035M gaussmeter and a HP 5350B microwave counter. An Oxford Cryostat ESR 900 was used for low-temperature studies. Cluster anions were generated for *in situ* EPR measurements by electrochemical reduction in THF/0.1 M Bu_4NPF_6 at 280 K (R_4Ga_4 cluster) and at temperatures ranging from 250 to 300 K (R_4In_4 cluster). A two-electrode EPR cell[6] with a platinum wire cathode was used; the potential was slowly increased until a typical constant electrolysis current of 10−25 μA was observed. EPR simulations were performed with a computer program based on a published algorithm[7] and further developed by Bruns.[8] Cyclic voltammetry was carried out at variable scan rates of 20−500 mV/s in THF/0.1 M Bu_4NPF_6 using a three-electrode configuration (glassy carbon or platinum working electrode, Pt counter electrode, Ag/AgCl reference) and a PAR 273 potentiostat and function generator. The ferrocenium/ferrocene couple $Fc^{+/0}$ served as internal reference.

Molecular Structure of Ga[C(SiMe$_3$)$_3$]

Structure Refinement. Beagley and Pritchard[9] have determined the gas-phase structure of the parent alkane, H*C*{Si(CH$_3$)$_3$}$_3$, and the present study follows their approach: Structure refinements were based on a molecular model of C_3 symmetry as indicated in Figure 2. Each Si(CH$_3$)$_3$ group was assumed to have C_3 local symmetry with the symmetry axis constrained to lie in the plane defined by the Si atom, the unique C atom which we designate by C*, and the Ga atom. We refer to the angle between the local symmetry axis and the C*−Si bond as the "tilt" and define it as positive, when the symmetry axis intersects the molecular symmetry axis *below* C* when the molecule is oriented as in Figure 2. The SiCH$_3$ fragments were assumed to have C_{3v} symmetry.

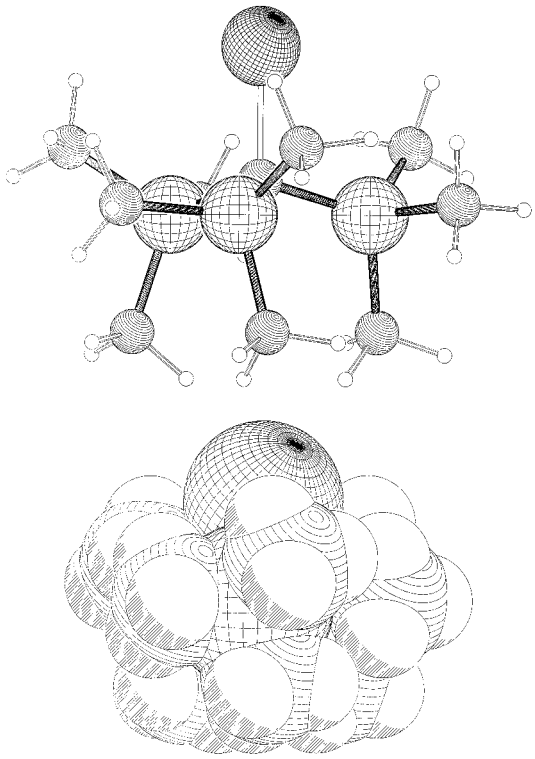

Figure 2. Ball-and-stick and space-filling molecular models (Pluton[28]) of GaC*{Si(CH$_3$)$_3$}$_3$. The molecular symmetry is C_3.

The molecular structure is then determined by 10 independent parameters, e.g. the Ga−C*, C*−Si, Si−C, and C-H bond lengths, the valence angles ∠GaC*Si, ∠CSiC, and ∠SiCH, two dihedral angles, τ(GaC*SiC) and τ(C*SiCH), and the tilt of the Si(CH$_3$)$_3$ groups. These parameters and 12 root-mean-square vibrational amplitudes (l) were refined by least-squares calculations on the modified molecular intensity data using the program KCED26 written by Gundersen, Samdal, Seip, and Strand.[10] During the refinements the 50 cm data were given unit weight, while each of the two 25 cm curves was assigned a weight of $W = 0.5$. The refinement converged to the values listed in Table 1. The estimated standard deviations listed in the table have been obtained from those calculated by the program by multiplication with a factor of 2.0 to compensate for data correlation[11] and further expanded to include an estimated scale uncertainty of 1.0 ppt.

The R-factor for the 50 cm/150 °C data,

$$R = [\sum W(I_{obs} - I_{calc})^2 / \sum W(I_{obs})^2]^{1/2}$$

was 3.9%, which shows that there is good agreement between observed and calculated intensities. The R-factor obtained for the 25 cm/200 °C data, however, was

(5) Bonham, R. A.; Schäfer, L. Complex Scattering Factors for the Diffraction of Electrons by Gases. In *International Tables for X-Ray Crystallography*; Ibers, J. A., Hamilton, W. C., Eds.; Kynoch Press: Birmingham, U.K., 1974; Vol. IV.
(6) Kaim, W.; Ernst, S; Kasack, V. *J. Am. Chem. Soc.* **1990**, *112*, 173.
(7) Oehler, U. M.; Janzen, E. G. *Can. J. Chem.* **1982**, *60*, 1542.
(8) Bruns, W. Ph.D. Thesis, University of Stuttgart, 1993.
(9) Beagley, B.; Pritchard, R. G. *J. Mol. Struct.* **1982**, *84*, 129.
(10) Gundersen, G.; Samdal, S.; Seip, H. M.; Strand, T. G. The Norwegian Electron Diffraction Group, Annual Report 1980, Oslo, 1981.
(11) Seip, H. M.; Strand, T. G.; Stolevik, R. *Chem. Phys. Lett.* **1969**, *3*, 617.

Table 1. Interatomic Distances (r_a), Root-Mean-Square Vibrational Amplitudes (l), Valence Angles ($\angle_a$), Dihedral Angles (τ_a), and $Si(CH_3)_3$ Group Tilt Angle (δ) in GaC*{$Si(CH_3)_3$}$_3$ and H*C*{$Si(CH_3)_3$}$_3$[a]

	GaC*{$Si(CH_3)_3$}$_3$		H*C*{$Si(CH_3)_3$}$_3$[b]	
	r_a	l	r_a	l
		Bond Distances		
Ga−C*	206.4(17)	6.2(21)		
C*−Si	188.2(16)	6.3(3)[c]	188.6(6)	6.5(2)[d]
Si−C	189.3(7)	6.3(3)[c]	187.3(2)	6.5(2)[d]
C−H	110.7(4)	8.2(5)	111.4(2)	10.9(3)
		Nonbonded Distances		
Ga- -Si	316(1)	11(1)		
Ga- -C	348(5)	20(10)[e]		
Ga- -C	397(3)	20(10)[e]		
Ga- -C	490(2)	14(2)[f]		
Si- -Si	313(3)	20(13)		10.0(4)
Si- -C	356, 367, 394, 409	20(10)[e]		29(2)
Si- -C	478, 482	14(2)[f]		12.8(7)
Si- -H	253.7(9)	12.2(8)		13.6(4)
C- -C	300(1)	12(6)[g]		8.2(5)[h]
C*- -C	315, 316, 319	12(6)[g]		8.2(5)[h]
C- -C	349−630	15(2)		13(2)
		Valence Angles		
∠GaC*Si	106.2(9)		∠H*C*Si	101.2(7)
∠SiC*Si	112.5(8)		∠SiC*Si	116.3(8)
∠CSiC	104.6(7)		∠CSiC	105.8(3)
∠SiCH	112.8(9)		SiCH	112.1(3)
		Torsional Angles		
τ(GaC*SiC)	43(2)		τ(H*C*SiC)	39.5(3)
τ(C*SiCH)	56(31)		τ(C*SiCH)	27(5)
$Si(CH_3)_3$ Tilt				
δ	1.2(13)		δ	1.9(6)
R-factor[i]	0.057			

[a] Interatomic distances and root-mean-square vibrational amplitudes in pm, angles in deg. Estimated standard deviations in parentheses in units of the last digit. [b] Reference 9. [c−h] Sets of amplitudes which were assumed equal. [i] $R = [\sum W(I_{obs} - I_{calc})^2/\sum W(I_{obs})^2]^{1/2}$.

8.0%, which is one or two percent higher than expected, and inspection of the difference curves in Figure 1 indicates a systematic difference between 50 and 25 cm data below $s = 100$ nm^{-1}. One possible explanation for the difference might be that the higher temperature leads to significantly larger vibrational amplitudes. This explanation may be ruled out, however, since least-squares calculations with unit weight for the 25 cm data and low weight for the 40 cm failed to improve the agreement between the 25 cm data and calculated intensities. The discrepancy between the 25 cm data on the one hand and the 50 cm data and the calculated intensity on the other hand may also be due to partial decomposition at the higher temperature. The structure parameters obtained in refinements with unit weight on the 25 cm data and low weight on the 50 cm data differed from those listed in Table 1 by less than one estimated standard deviation. We believe, therefore, that the uncertainty introduced by the 25 cm/200 °C data are covered by the quoted esd values. Experimental molecular intensity curves and radial distribution curves are compared to their calculated counterparts in Figures 1 and 3, respectively.

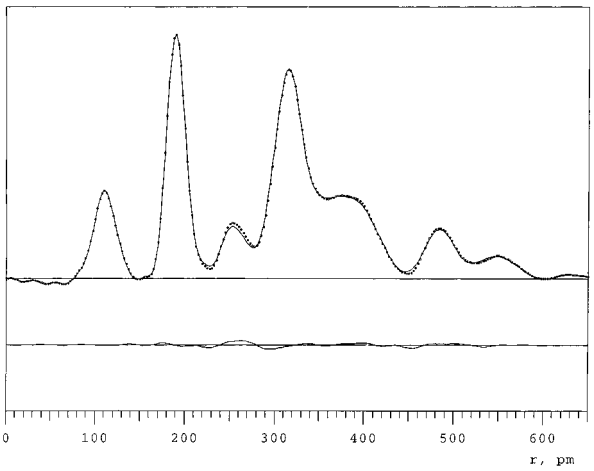

Figure 3. Experimental (dots) and calculated (lines) radial distribution curves for GaC*{$Si(CH_3)_3$}$_3$. The vertical scale is arbitrary. Below: Difference curves. Artifical damping constant $k = 25$ pm^2.

Discussion. The best values for the structure parameters of GaC*{$Si(CH_3)_3$}$_3$ ("Ga−R") are listed in Table 1. A sketch of the molecule is shown in Figure 2. To our knowledge GaR is the first monomeric alkyl derivative of a monovalent group 13 element to be structurally characterized, and the magnitude of the Ga−C bond length is of particular interest. GaR is a very congested molecule, and the mean Si−C bond length, 189.0(2) pm, is 1.5 pm larger than the reference Si−C bond length in $Si(CH_3)_4$, 187.5(2) pm.[12] If we assume that congestion leads to a similar elongation of the Ga−C* bond, we obtain an estimated reference value of 205 pm for an unstrained Ga(I)−C bond. There is thus no doubt that a Ga(I)−C single bond is inherently longer than a Ga(III)−C single bond; the bond length in $Ga(CH_3)_3$ is 196.7(2) pm.[13]

Similarly the Ga(I)−Cl bond length in gaseous GaCl, 220.2 pm, is significantly longer than the Ga(III)−Cl bond length in gaseous, monomeric $GaCl_3$, 210.8(3) pm.[14] The difference has been rationalized as a hybrid-

(12) Beagley, B.; Monaghan, J. J.; Hewitt, T. G. *J. Mol. Struct.* **1971**, *8*, 401.
(13) Beagley, B.; Schmidling, D. G.; Steer, I. A. *J. Mol. Struct.* **1974**, *21*, 437

ization effect: While Ga(I) may use an unhybridized *p* orbital for bond formation, the Ga(III) atoms in $GaCl_3$ or $Ga(CH_3)_3$ are presumably sp^2 hybridized. Though the Ga(I)−Cl bond is longer than the Ga(III)−Cl bond, it is also stronger: the dissociation energy of Ga−Cl is 475 kJ mol^{-1}, and the mean bond energy in $GaCl_3$ is 355 ± 5 kJ mol^{-1}.[14] We have suggested that the difference is due to the energy required to promote the Ga atom from an $(s)^2(p)^1$ to an $(s)^1(p)^2$ electron configuration. If this explanation is correct, a Ga(I)−C bond should also be stronger than a Ga(III)−C bond.

The structure parameters of the parent alkane, H*C*-{Si(CH$_3$)$_3$}$_3$, are listed in Table 1 for comparison.[9] Replacement of the unique H atom (H*) by a more voluminous Ga atom leads to an opening of the ∠GaC*Si angle to 106.2(9)° as compared to the ∠H*C*Si angle of 101.2(7)° in the alkane. At the same time, the ∠SiC*Si angles are reduced from 116.3(4)° in the alkane to 112.5(8)° in the metal alkyl. The angles ∠GaC*Si and ∠SiC*Si are in fact similar to the corresponding angles in BrC*{Si(CH$_3$)$_3$}$_3$.[15] The structure of the gallium alkyl is otherwise indistinguishable from that of the parent alkane.

The In_4 analogue **2** decomposes at 150 °C, and an attempt to get the gas-phase data from **2** led to complete decomposition under deposition of elemental indium and the formation of $HC(SiMe_3)_3$ as the only volatile compound. The molecular structures of monomeric monocyclopentadienyl compounds with the heavier third main group elements in unusual oxidation states (e.g. Al^{I}(C$_5$Me$_5$),[16] Ga^{I}(C$_5$Me$_5$),[17] In^{I}(C$_5$Me$_5$),[18] and Tl^{I}(C$_5$Me$_5$)[19]) have already been determined by electron diffraction in the gas phase. They all are much more volatile than the cluster compounds **1** or **2**. With the η^5-cyclopentadienyl groups the central atoms can obey the octet rule by the interaction with the six π-electrons of the ligand, in contrast to Ga[C(SiMe$_3$)$_3$], which exhibits strong coordinative and electronic unsaturation.

Electrochemistry and EPR of the Cluster Compounds

Results. The compounds R_4Ga_4 and R_4In_4 were subjected to cyclic voltammetry at glassy carbon or platinum electrodes in THF/0.1 M Bu_4NPF_6 at variable scan rates (20−500 mV/s). Both compounds are reversibly reduced, at −1.98 V (Ga tetramer, Figure 4) and −1.99 V vs ferrocenium/ferrocene (In tetramer). The cyclic voltammetric response does not significantly depend on the electrode material (C or Pt); we shall thus refer only to the data obtained with glassy carbon. Not only the redox potential values but also the peak current ratios (1.00 ± 0.05) and the peak potential differences ΔE_{pp} are quite similar for the first reduction processes

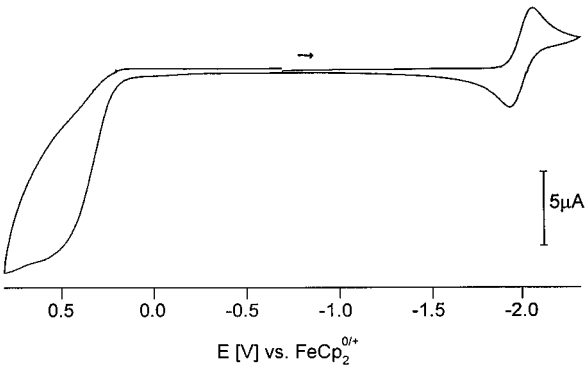

Figure 4. Cyclic voltammogram of R_4Ga_4 in THF/0.1 M Bu_4NPF_6 at 100 mV/s scan rate.

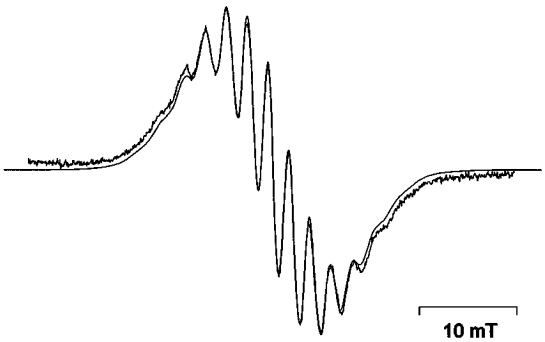

Figure 5. Experimental and computer-simulated EPR spectrum of $[(RGa)_4]^{\bullet-}$ as generated by electrochemical reduction in THF/0.1 M Bu_4NPF_6 at 280 K. Simulation parameters: Four equivalent gallium centers, $a(^{69}Ga)$ = 1.93 mT, $a(^{71}Ga)$ = 2.45 mT, 1.3 mT line width.

of both cluster molecules; at 100 mV/s scan rate ΔE_{pp} is 90 mV for Ga_4R_4 and 98 mV for R_4In_4. For the latter compound, the ΔE_{pp} value increases from 88 mV at 20 mV/s scan rate to 134 mV at 500 mV/s scan rate. Multiple scans show no changes in the appearance of the first reduction waves.

Further reduction processes occurring at about −3.0 V (R_4Ga_4) or −2.8 V vs $Fc^{+/0}$ (R_4In_4) are irreversible, as is the electrochemical oxidation at about +0.25 V (R_4In_4) or +0.8 V vs $Fc^{+/0}$ (R_4Ga_4, Figure 4).

Whereas the anion radical $[R_4Ga_4]^{\bullet-}$ gave an easily detectable EPR spectrum (Figure 5), all attempts to obtain an EPR signal from $[R_4In_4]^{\bullet-}$ failed, despite careful *in situ* electrolyses at ambient temperature and low temperatures (250 K) and EPR measurements down to 4 K. The reduced complex $[R_4Ga_4]^{\bullet-}$, on the other hand, exhibits a partially resolved EPR spectrum (Figure 5) at g = 2.0023 which can be perfectly simulated assuming the coupling of one unpaired electron with *four equivalent* gallium nuclei in natural abundance (^{69}Ga: 60.1%, $I = {}^3/_2$, g_N = 1.3444. ^{71}Ga: 39.9%, $I = {}^3/_2$, g_N = 1.7082).[20,21]

Assuming the natural isotopic composition, we arrive at coupling constants of $a(^{69}Ga)$ = 1.930 mT and $a(^{71}Ga)$ = 2.451 mT from the computer simulation. The error margin within which the four gallium centers are equivalent is estimated at about ±0.5 mT for each isotope; within that margin, the two gallium isotopes

(14) Haaland, A.; Hammel, A.; Martinsen, K.-G.; Tremmel, J.; Volden, H. V. *J. Chem. Soc., Dalton Trans.* **1992**, 2209 and references therein.
(15) Brain, P. T.; Metha, M.; Rankin, D. W. H.; Robertson, H. E.; Eaborn, C.; Smith, J. D.; Webb, A. D. *J. Chem. Soc., Dalton Trans.* **1995**, 349.
(16) Haaland, A.; Martinsen, K. G.; Shlykov, S. A.; Volden, H. V.; Dohmeier, C.; Schnöckel, H. *Organometallics* **1995**, *14*, 3116.
(17) Haaland, A.; Martinsen, K.-G.; Volden, H. V.; Loos, D; Schnöckel, H. *Acta Chem. Scand.* **1994**, *48*, 172.
(18) Beachley, O. T., Jr.; Blom, R.; Churchill, M. R.; Faegri, K., Jr.; Fettinger, J. C.; Pazik, J. C.; Victoriano, L. *Organometallics* **1989**, *8*, 346.
(19) Blom, R.; Werner, H.; Wolf, J. *J. Organomet. Chem.* **1988**, *354*, 293.
(20) Weil, J. A.; Bolton, J. R.; Wertz, J. E. *Electron Paramagnetic Resonance*; Wiley: New York, 1994.
(21) There are five isotope combinations: $(^{69}Ga)_4$ (13.1%), $(^{69}Ga)_3(^{71}Ga)$ (34.7%), $(^{69}Ga)_2(^{71}Ga)_2$ (34.5%), $(^{69}Ga)(^{71}Ga)_3$ (15.3%), and $(^{71}Ga)_4$ (2.5%).

appear undifferentiated so that four equivalent nuclei of $I = {}^3/_2$ produce a 13-line spectrum in the first approximation (number of lines $N = 2nI + 1$, n = number of equivalent nuclei). Nevertheless, the good fit of the intensity distribution (Figure 5) shows that the assumed hyperfine splitting according to a formulation $[(RGa)_4]^{\bullet-}$ is also valid at a more refined level.

Discussion. The gallium and indium clusters are reversibly reduced at virtually identical potentials which appears to suggest a rather similar electronic structure involving a cluster orbital[22] as lowest unoccupied MO (LUMO). The reduction occurs in a less negative potential region where extended organic π systems such as anthracene or benzophenone also accept an additional electron. Both the (irreversible) oxidation and second reduction[23] seem to be easier for the indium derivative, in agreement with the notion of a diminished stability of the heavier metal cluster.

Despite the almost identical redox potentials and reversibility features, the two cluster anions exhibit an unexpectedly different EPR response. Whereas the reduced gallium cluster displays a normal EPR spectrum, the *in situ* electrochemical reduction of In_4R_4 under identical conditions or at even lower temperatures did not produce a detectable EPR signal between 4 and 300 K in THF/0.1 M Bu_4NPF_6. This can have several causes: There could be extreme EPR line-broadening for this anion radical of a heavy metal cluster due to rapid relaxation as caused by the presence of close-lying excited states in connection with strong spin−orbit coupling contributions. The lowest unoccupied cluster MO is likely to be an e(π) or another degenerate orbital (in T_d symmetry),[22] and its occupation by one electron may result in a more or less pronounced distortion to remove the degeneracy. Distortion can produce excited states lying close to the doublet ground state which may be responsible for rapid relaxation and the absence of detectable EPR intensity.[20] In addition, the results for the gallium analogue suggest very extensively spread ^{115}In hyperfine splitting (95.7% natural abundance, $I = {}^9/_2$, $g_N = 1.2313$)[20] for $[(RIn)_4]^{\bullet-}$ with 37 theoretical lines spaced at more than 3 mT; the resulting total spectral width would then exceed 100 mT which might also contribute to the lack of a detectable EPR signal.

In contrast, the monoanionic tetrakis(organogallium) cluster exhibits an EPR spectrum which can be simulated within the above mentioned line width limitation by assuming the coupling of the unpaired electron with four equivalent or virtually equivalent metal centers. It may be speculated that the extent (or type) of distortion from (spectroscopic) T_d symmetry is different for $[(RIn)_4]^{\bullet-}$ and $[(RGa)_4]^{\bullet-}$, resulting in a complete spin delocalization over the four gallium centers for the latter system (valence averaging, formal oxidation state +0.75).[24]

The size of about 2 mT for the coupling constant from *four* equivalent metal centers supports this notion. Whereas the metal hyperfine splitting of the dinuclear gallium-centered anion radicals $[(R_2Ga)_2]^{\bullet-}$ (R = aryl, alkyl) lies between 3 and 7 mT,[25] mono- and dinuclear gallium compounds of radical ligands exhibit generally smaller values of $a(^{69,71}Ga)$.[26] The high spectroscopic symmetry of the cluster radical $[(RGa^{0.75})_4]^{\bullet-}$ as evident from the hyperfine splitting is also supported by the isotropic g factor which happens to coincide with that of the free electron ($g = g_e = 2.0023$) despite the contribution from four gallium nuclei. An $Al_6(CMe_3)_6$ radical anion has recently been postulated from EPR spectroscopic results by the groups of Schnöckel and Ahlrichs.[27]

Acknowledgment. We are grateful to the VISTA program of STATOIL, the Norwegian Academy of Science and Letters, the Deutsche Forschungsgemeinschaft, and the Fonds der Chemischen Industrie for financial support.

OM950755S

(22) See: Schneider, U.; Ahlrichs, R.; Horn, H.; Schäfer, A. *Angew. Chem.* **1992**, *104*, 327; *Angew. Chem., Int. Ed. Engl.* **1992**, *31*, 353 and literature therein.

(23) The dianions $[(RM)_4]^{2-}$ would conform to the Wade rules: Wade, K. *Adv. Inorg. Chem. Radiochem.* **1976**, *18*, 1.

(24) For a discussion of one spin in a degenerate orbital see EPR studies of the benzene radical ions: Gerson, F. *High Resolution E.S.R. Spectroscopy*; Wiley/Verlag Chemie: London/Weinheim, 1970; p 112 and literature cited.

(25) (a) Uhl, W.; Schütz, U.; Kaim, W.; Waldhör, E. *J. Organomet. Chem.* **1995**, *501*, 79. (b) He, X.; Bartlett, R. A.; Olmstead, M. M.; Ruhlandt-Senge, K.; Sturgeon, B. E.; Power, P. P. *Angew. Chem.* **1993**, *105*, 761; *Angew. Chem., Int. Ed. Engl.* **1993**, *32*, 717.

(26) (a) Kaim, W. *Z. Naturforsch. B* **1982**, *37*, 783. (b) Kaim, W.; Matheis, W. *J. Chem. Soc., Chem. Commun.* **1991**, 597. (c) Hasenzahl, S.; Kaim, W.; Stahl, T. *Inorg. Chim. Acta* **1994**, *225*, 23.

(27) Dohmeier, C.; Mocker, M.; Schnöckel, H.; Lötz, A.; Schneider, U; Ahlrichs, R. *Angew. Chem.* **1993**, *105*, 1491; *Angew. Chem., Int. Ed. Engl.* **1993**, *32*, 1428.

(28) Spek, A. L. The Euclid Package. In *Computational Crystallography*; Sayre, D., Ed.; Clarendon: Oxford, U.K., 1982.